Journal of
Manufacturing and Materials Processing

MDPI

Article

A Comprehensive Study on the Optimization of Drilling Performance in Hybrid Nano-Composites and Neat CFRP Composites Using Statistical and Machine Learning Approaches

Tanzila Nargis [1], S. M. Shahabaz [2], Subash Acharya [2,*], Nagaraja Shetty [2,*], Rashmi Laxmikant Malghan [3] and S. Divakara Shetty [4]

1 Department of Information Science and Engineering, NMAM Institute of Technology, NITTE (Deemed to be University), Karkala 574110, India; tanzilanargis@nitte.edu.in
2 Department of Mechanical & Industrial Engineering, Manipal Institute of Technology, Manipal Academy of Higher Education, Manipal 576104, India; shahabaz.sm@learner.manipal.edu
3 Department of Data Science and Computer Applications, Manipal Institute of Technology, Manipal Academy of Higher Education, Manipal 576104, India; rashmi.malghan@manipal.edu
4 Alva's Institute of Engineering and Technology, Mijar, Moodabidri, Mangalore 574225, India
* Correspondence: subash.acharya@manipal.edu (S.A.); nagaraj.shetty@manipal.edu (N.S.)

Abstract: Carbon fiber-reinforced polymer (CFRP) composites have gradually replaced metals due to their exceptional strength-to-weight ratio compared to metallic materials. However, the drilling process often reveals various defects, such as surface roughness, influenced by different drilling parameters. This study explores the drilling quality of uni-directional CFRP composites, as well as hybrid Al_2O_3 alumina and hybrid SiC silicon carbide nano-composites, through experimental exploration using step, core, and twist drills. Response surface methodology (RSM) and statistical tools, including main effect plots, ANOVA, contour plots, and optimization techniques, were used to analyze the surface roughness of the hole. Optimization plots were drawn for optimal conditions, suggesting a spindle speed of 1500 rpm, feed of 0.01 mm/rev, and a 4 mm drill diameter for achieving minimum surface roughness. Furthermore, two machine learning models, artificial neural network (ANN) and random forest (RF), were used for predictive analysis. The findings revealed the robust predictive capabilities of both models, with RF demonstrating superior performance over ANN and RSM. Through visual comparisons and error analyses, more insights were gained into model accuracy and potential avenues for improvement.

Keywords: carbon fiber-reinforced polymer; drilling; response surface methodology; artificial neural network; random forest

Citation: Nargis, T.; Shahabaz, S.M.; Acharya, S.; Shetty, N.; Malghan, R.L.; Shetty, S.D. A Comprehensive Study on the Optimization of Drilling Performance in Hybrid Nano-Composites and Neat CFRP Composites Using Statistical and Machine Learning Approaches. *J. Manuf. Mater. Process.* **2024**, *8*, 67. https://doi.org/10.3390/jmmp8020067

Academic Editors: Patricia Krawczak and Ludwig Cardon

Received: 19 February 2024
Revised: 20 March 2024
Accepted: 21 March 2024
Published: 29 March 2024

1. Introduction

Among the various classifications of composites, carbon fiber-reinforced polymer (CFRP) has garnered considerable attention in aerospace circles owing to its exceptional property of offering a high strength-to-weight ratio [1]. The substantial weight of engine components in automobiles increases fuel consumption, diminishing efficiency. Consequently, replacing these components with composite materials has been shown to enhance overall performance [2]. Similarly, weight reductions of 25% have been observed for both commercial and military aircraft structures, respectively. Notably, in the case of the Boeing 777, a prominent passenger aircraft constructed primarily of carbon fiber epoxy, weight savings of 15–20% have been achieved. Components fabricated from composites in the Boeing 777 include flaperons, ailerons, inboard and outboard flaps, landing gear doors, and engine cowlings [3].

There has been a notable surge in demand for advanced composites with enhanced performance characteristics in recent years. Nano-composites represent a cutting-edge category of materials wherein one or more distinct nanoparticles are incorporated into the matrix material to further augment performance [4]. Epoxy resin, derived from the interaction of bisphenol A and epichlorohydrin, has served as a primary matrix material for the fabrication of these nano-composites for many years [5]. Nano-composites comprising epoxy and nanoparticle reinforcements have exhibited exceptional mechanical, thermal, and electrical properties. Key factors such as molecular structure, curing conditions, and the ratio of epoxy resin to curing agent(s) significantly influence their performance. Nanoparticles are characterized by a high surface area, rendering them invaluable across numerous applications [6]. Inorganic particles such as alumina (Al_2O_3) and silicon carbide (SiC) show high hardness, excellent wear, and temperature resistance, as well as satisfactory chemical inertness, making them extensively utilized in metallurgical components, composite fabrication, and electronic industries [7,8].

In a study conducted by Mohanty et al. [9], it was found that incorporating Al_2O_3 nanoparticles into hybrid carbon and glass fiber-reinforced composites significantly enhanced both tensile strength and modulus. Similarly, Priyadarshi et al. [10] investigated the mechanical characteristics of Al_2O_3-filled jute epoxy composite under various conditions, revealing notable improvements such as heightened impact strength (1.902 Joules), augmented flexural strength (72.94 MPa), and a maximum hardness reaching 29.9 Vickers hardness number. Additionally, the authors, in their prior work, reported experimental results on the enhancement of mechanical properties at different nano-filler loadings (Al_2O_3 and SiC) in neat CFRP composite compared to hybrid nano-composites. The maximumHighest mechanical properties were observed at 1.75 wt.% filler loading for Al_2O_3 hybrid nano-composites and at 1.25 wt.% filler loading for SiC hybrid nano-composites [11,12].

Defects such as fiber pull-out, debonding, microcracking, surface roughness, and delamination occur in the drilled holes after drilling. To determine the extent of drilling-induced damage, researchers have used a wide range of methods, such as digital image processing, optical microscopy, C-scan, X-ray, and laser-based imaging, to scan electron microscopic images. The Taguchi technique and analysis of variance (ANOVA) have been used in experimental studies, including those conducted by Davim and Reis, [13] to establish a correlation between surface roughness, feed rate, and cutting speed. Tsao et al. [14] also suggested that the right tool geometry and cutting parameters might decrease surface roughness in CFRP composite drilling. Response surface methodology (RSM) is a straightforward and efficient method for establishing a relationship between output variables and machining parameters [15]. RSM was utilized by Palanikumar and Davim [16] to forecast surface roughness in glass fiber-reinforced polymer (GFRP) composite drilling.

Soft computing techniques serve as valuable supplements to conventional statistical methods in the analysis of composite drilling processes. Their utilization in this context aims to tackle the intricate, nonlinear, and ambiguous aspects inherent in process variables. Through soft computing modeling, researchers can rely on a robust approach that consistently yields thorough, accurate, and dependable results. Recently, researchers have been using various soft computing techniques, including response surface methodology (RSM) [17], random forest technique (RF) [18], artificial neural network (ANN) [19], and design of experiments (DOE) [20]. These methods provide researchers with versatile tools to navigate the complexities of the drilling process in composites.

Given the typically extensive and high-cost nature of experiments required to assess the machinability of metals or materials, an effective approach lies in the utilization of statistically or numerically designed tests, commonly known as design of experiments (DOE). This methodology enables researchers to strategically plan experimental set-ups, evaluate the impact of each process parameter, and ultimately minimize the total number of tests needed to achieve optimal conditions [21].

Jayabal and Natarajan [22] conducted a study to investigate the influence of process parameters, including drill diameter, spindle speed, and feed rate, on thrust force, torque, and tool wear during the drilling of coir fiber-reinforced composite materials. Utilizing the Box–Behnken design and genetic algorithm (GA) techniques, the researchers were able to identify the optimal process parameters. Their findings indicated that this approach was effective in forecasting both main and interaction effects and drilling process output variables. Moreover, it facilitated the determination of optimal values for drilling parameters. Therefore, Jayabal and Natarajan concluded that the employed technique demonstrated practicality in optimizing the drilling process. To predict the delamination and surface roughness during the drilling of CFRP composite, Enemuoh et al. [23] employed a multilayered perceptron neural network (MLPNN) model. They discovered that the predicted and experimental results for delamination and surface roughness agreed well. Similarly, to optimize the drilling process output variables during the drilling of the Al/SiCp composite, Karthikaya et al. [24] applied fuzzy logic and genetic algorithm techniques. The experimental data were trained and simulated using fuzzy logic, and the GA model was utilized to optimize the process parameters.

It is evident from the literature that the appropriate machining parameters and tool geometry can lessen drilling-induced damage to CFRP composites. In order to measure the output variable surface roughness (R_a), this study examines the drilling of hybrid nano-composites composed of Al_2O_3, as well as SiC at different cutting parameters (spindle speed, feed, drill diameter, and drill type). Surface roughness is a crucial factor in machining processes, influencing product quality and performance of composites. Accurate prediction models can aid in optimizing machining parameters for desired surface finish. In this study, along with the experimental and RSM results, two popular machine learning models are implemented—artificial neural network (ANN) and random forest (RF)—for predicting R_a in different materials, like Al_2O_3, SiC, and neat CFRP composites. The implemented models (ANN, RF) are evaluated based on prediction accuracy, that is, relative error attained for R_a. Later, a comparative analysis is made against the R_a values obtained from response surface methodology (RSM) with ANN and RF. RSM is employed to design experiments with different machine parameters, and main effects plots, contour plots, and optimization plots aregenerated using experimental results.

2. Material and Methods

2.1. Materials

In this investigation, an unidirectional carbon fiber-reinforced polymer (CFRP) material has been employed as a reinforcing agent, along with the utilization of bisphenol-A epoxy resin and an amine-based hardener serving as the polymer matrix. To enhance the structural attributes, distinct inorganic nano-fillers, namely Al_2O_3 and SiC, were carefully incorporated at varying filler loadings (1, 1.5, 1.75, 2 wt% for Al_2O_3 and 1, 1.25, 1.5, 2 wt% for SiC), yielding hybrid nano-composites. The achievement of a homogenous dispersion of nano-fillers was methodically accomplished through a combined application of sonication and magnetic stirring methods.

The manufacturing process encompassed the fabrication of both the CFRP and hybrid nano-composites through a hand lay-up method, succeeded by a compression molding technique with a curing duration of 24 h at room temperature. The drilling was performed utilizing a computer numerical control vertical machining center, as represented in Figure 1. The maximum properties obtained for hybrid nano-composites were at 1.75 wt% for Al_2O_3 hybrid nano-composites and at 1.25 wt% for SiC hybrid nano-composites, as reported by authors in their previous work. Drilling was performed for the above hybrid nano-composites, and their surface roughness was measured.

2.2. Machining Parameters

Table 1 illustrates the selected machining parameters chosen for the investigation. An experimental design incorporating response surface methodology (RSM) through Minitab V15 software was employed, utilizing the following machining parameters. Composite strips measuring 250 mm × 25 mm were precisely cut using an abrasive water jet cutting machine. A total of 180 holes were drilled, with 60 holes dedicated to each composite type. Three types of drill geometry were selected, i.e., twist drill, step drill, and core drill, as shown in Figure 2. The drill bits were made of solid carbide material, and a diamond coating was applied using the physical vapor deposition (PVD) method. The PVD diamond coating provides a higher tool life and improved quality of drilled holes. Also, it provides resistance to oxidation, corrosion, and wearing of tools. PVD diamond coating was performed by exposing the cutting tool to the vapor of coating material at higher temperatures, up to 1000 °C, and then allowing it to adhere to the cutting tool.

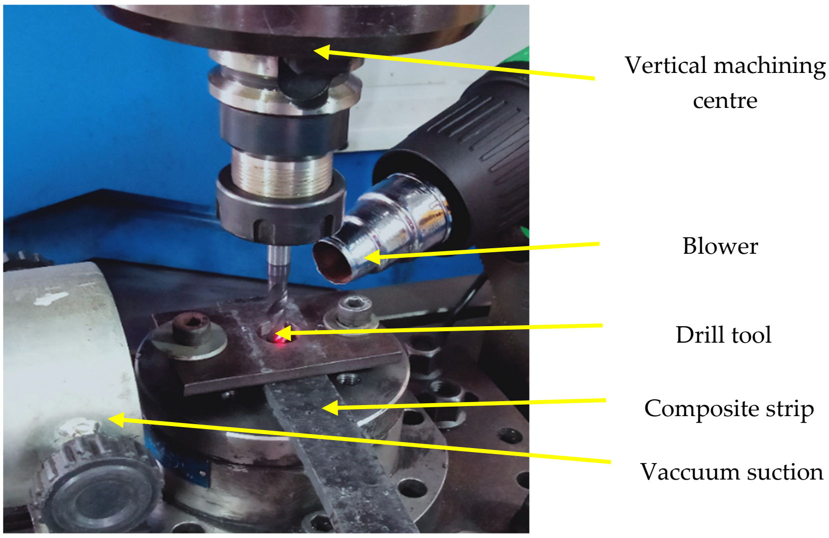

Figure 1. Schematic representation of drilling set-up.

Table 1. Various machining parameters selected for drilling.

Sl. No.	Parameters			
	Spindle Speed (rpm)	Feed (mm/rev)	Drill Diameter (mm)	Drill Type
1	1500	0.01	4	Twist
2	3500	0.02	6	Step
3	5500	0.03	8	Core

Figure 2. Drill types with PVD coating.

2.3. Surface Roughness Measurement

The surface roughness (R_a) of the drilled hole was measured by using the Taylor-Hobson Surtronic 3+ instrument (Model: Surtronic 3+, Taylor Hobson Ltd., Leicester, UK), as shown in Figure 3. Surface roughness was measured at six different locations with a probe speed of 0.5 mm/s in the transverse direction, up to 4 mm in length. The average surface roughness value was noted to determine the surface quality of the hole wall.

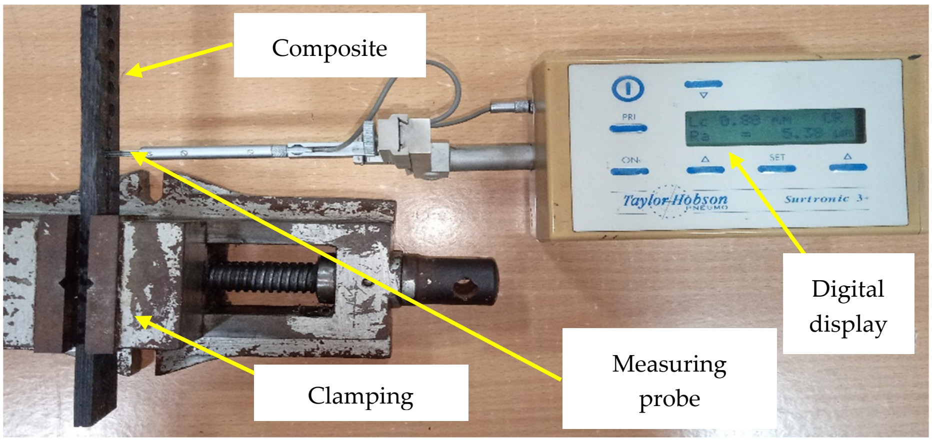

Figure 3. Measurement of surface roughness of the drilled hole.

2.4. Statistical Tools

RSM serves as a predictive and optimization tool for output variables affected by multiple factors. The modeling and analysis of data involved the application of RSM employing a full factorial method. An empirical connection between process parameters was established using RSM's central composite design (CCD). Equation (1) illustrates the correlation between various output parameters ('y'), such as delamination factor, burr area, surface roughness, and hole temperature, and the corresponding process parameters (spindle speed (A), feed (B), drill diameter (C), and type of drill (D).

$$y = \beta_o + \beta_1 A + \beta_2 B + \beta_3 C + \beta_4 D + \beta_5 A^2 + \beta_6 B^2 + \beta_7 C^2 + \beta_8 D^2 + \beta_9 AB + \beta_{10} AC + \beta_{11} AD + \beta_{12} BC + \beta_{13} BD + \beta_{14} CD + \varepsilon \quad (1)$$

where, β_0, β_1, β_2, . . ., β_{14} are the regression coefficients and ε is the random error.

This study also employed analysis of variance (ANOVA) to assess the impact of process parameters on the output variables of the drilling process in both the hybrid nano-composites and the neat CFRP composite. The objective of ANOVA is to identify the factors and their combinations that have a substantial influence on the machining operation. The analysis was conducted with a significance level set at $\alpha = 0.05$, corresponding to a confidence level of 95%. Similarly, the impact of different process parameters on surface roughness values was assessed using main effects plots and contour plots. A main effects plot illustrates the mean response values for each level of a process parameter, allowing for a clear understanding of its influence. Comparatively, the main effects plot enables the assessment of the relative intensity of the impacts of various factors. Likewise, contour plots offer a 2D surface projection to depict the variation in response. These plots are generated by simultaneously considering two input factors while maintaining the remaining factors at their median values. The resulting contour lines connect data points with identical response values, providing a comprehensive visualization of the surface's behavior.

2.5. Optimization of Process Parameters Using RSM

The process parameters were optimized through response surface methodology (RSM). In RSM, the desirability function method is commonly employed for the optimization of multi-output variables. According to this methodology, any process exhibiting a quality characteristic beyond the acceptable limits is considered entirely unacceptable. The primary objective was to identify process parameters that yield the most favorable output variables. In this investigation, the desirability function approach was utilized to optimize the output variable within the framework of RSM. The desirability function transforms the output variable, specifically the surface roughness value, into a dimensionless variable known as the desirability index (d_i), as defined in Equation (2). The desirability index ranges within the closed interval of (0, 1). A higher desirability index value for output variable indicates a greater contribution to the overall performance by the respective output variable. The desirability index (d_i) is a function of the output variables (y_i), and each individual desirability function assigns a number between 0 and 1, where 0 signifies undesirability and 1 signifies a desirable or ideal value for the output variable.

$$d_i = \left(\frac{y - y_{min}}{y_{target} - y_{min}}\right)^q \quad y_{min} < y < y_{target} \tag{2}$$

In Equation (2), the output variable y is represented, where y_{min} corresponds to the lowest value, y_{target} denotes the target values, and q stands for the weight. The weight q can assume either low value ($0 < q < 1$) or high value ($q > 1$), depending on the desired effect. A value of one produces a linear ramp function between the low, target, and high values. Increasing the weight facilitates moving the result closer to the desired goal. The comprehensive assessment of product performance involves calculating the geometric mean of all desirability indices to derive an aggregate (global or composite) desirability index D, as expressed in Equation (3).

$$D = (d_1 \times d_2 \times d_3 \ldots \ldots d_m)^{1/m} \tag{3}$$

In Equation (3), the desired output variable is denoted as 'm'. An association is established between the output responses and the various process or machining factors through the incorporation of a second-degree polynomial regression equation into the experimental data. Subsequently, the determination of the output variable's desirability is executed to gauge the overall desirability. To identify the optimal overall desirability, the univariate search method is applied, systematically exploring diverse combinations of machining factors within the specified experimental range.

2.6. Prediction Methods

2.6.1. Artificial Neural Network (ANN)

ANN is a brain-structured computation model. The structure of neurons provides the computing capability to identify the relations between the input and the output parameters through the mapping model. The ANN structure consists of 3 layers:

- Input layer: number of input parameters = number of neurons placed in the input layer.
- Hidden layer: a greater number of neurons placed compared to the input layer.
- Output layer: number of output parameters = number of neurons.

A relation will be created by flowing the information between the input layer to the hidden layer and from the hidden to the output layer. The forward and back propagation techniques can be implemented for each iteration, that is, for the input–output pair. In the case of backpropagation, initially, the result "Y" will be calculated. Then, if the desired results are not met, the weight adjustment needs to be performed backward from the output layer to the hidden layer and from the hidden layer to the input layer.

2.6.2. Random Forest (RF)

Random forest (RF) is an effective algorithm that fits the ensemble learning family. It outperforms individual decision trees. RF involves building multiple decision trees, and later, it combines their predictions. The significance of RF is a measure of feature importance based on the contribution of each feature involvement in reducing impurity (error) across all the developed trees. This flow helps in parameter tuning, interpreting results, and identifying the insights, thus leading to flexible handling of various kinds of data. RF supports the parallelization making the training faster as each tree developed is independent. In the case of prediction, the individual trees are averaged to attain the final outcome.

3. Results and Discussion

It is well known that surface roughness is one of the key parameters that decide the quality of the drilled holes and the cost of production. It largely depends on the kind of material to be drilled, the drill type to be used, and its cutting speed, feed, and the cutting force produced in drilling. Table 2 represents the regression equations for hybrid nano-composites and the neat CFRP composite for each drill type.

Table 2. Regression equations from RSM.

Composite Type	Drill Type	Regression Equation
Al_2O_3 hybrid nano-composite	Twist	0.9415 + 0.00.020018 × SS + 1.36 × F + 0.06897 × DD − 0.000000×S×SSS − 9. 4 × F × F − 0.002027 × DD × DD + 0.000088 × SS × F − 0.000001 × SS × DD − 0.1000 × F × DD
	Step	0.8863 + 0.000014 × SS + 1.36 × F + 0.06112 × DD − 0.000000 × SS × SS − 9.4 × F × F − 0.002027 × DD × DD + 0.000088 × SS × F − 0.000001 × SS × DD − 0.1000 × F × DD
	Core	1.1867 + 0.000016 × SS + 1.05 × F + 0.06012 × DD − 0.000000 × SS × SS − 9.4 × F × F − 0.002027 × DD × DD + 0.000088 × SS × F − 0.000001 × SS × DD − 0.1000 × F × DD
SiC hybrid nano-composite	Twist	1.1715 + 0.000011 × SS + 0.98 × F + 0.04702 × DD + 0.000000 × SS × SS − 1.5 × F × F − 0.000788 × DD × DD + 0.000010 × SS × F + 0.000000 × SS × DD + 0.0021 × F × DD
	Step	1.1656 + 0.000008 × SS + 0.66 × F + 0.03712 × DD + 0.000000 × SS × SS − 1.5 × F × F − 0.000788 × DD × DD + 0.000010 × SS × F + 0.000000 × SS × DD + 0.0021 × F × DD
	Core	1.4042 + 0.000010 × SS + 0.97 × F + 0.04317 × DD + 0.000000 × SS × SS − 1.5 × F × F − 0.000788 × DD × DD + 0.000010 × SS × F + 0.000000 × SS × DD + 0.0021 × F × DD
Neat CFRP composite	Twist	1.5652 + 0.000021 × SS + 1.23 × F + 0.07933 × DD − 0.000000 × SS × SS + 8.9 × F × F − 0.001777 × DD × DD + 0.000015 × SS × F − 0.000001 × SS × DD − 0.0479 × F × DD
	Step	1.3385 + 0.000020 × SS + 1.08 × F + 0.06688 × DD − 0.000000 × SS × SS + 8.9 × F × F − 0.001777 × DD × DD + 0.000015 × SS × F − 0.000001 × SS × DD − 0.0479 × F × DD
	Core	1.8969 + 0.000023 × SS + 1.10 × F + 0.07738 × DD − 0.000000 × SS × SS + 8.9 × F × F − 0.001777 × DD × DD + 0.000015 × SS × F − 0.000001 × SS × DD − 0.0479 × F × DD

From Table 3, it is observed that the surface roughness decreases with the addition of nanoparticles. The minimum surface roughness was noted for the Al_2O_3 hybrid nano-composite with an R_a value of 1.598 µm, followed by the SiC hybrid nano-composite with an R_a value being 1.783 µm, respectively. In contrast, the maximum R_a was observed for neat the CFRP composite (2.533 µm). This represents that the nanoparticle acts as a lubricant during the drilling of the composite by reducing the friction occurring at the tool–workpiece interaction. Furthermore, as declared in the previous work of the authors, it is proven that the addition of nanoparticles improves chemical bonding with polymer resin. The chemical bonding energy of oxygen atoms of Al_2O_3 with the hydrogen atoms of polymer chains is greater compared to the carbon atom of SiC combining with hydrogen atoms of polymer chains [11,12]. This good bonding between nanoparticles and resin molecules has shown improved mechanical properties of the hybrid nano-composites further indicating improved surface finish observed for hybrid nano-composites compared to the neat CFRP composite, as noted from Table 3. Also, from Table 3, the standard deviation values are less than 1, demonstrating that all the datasets are closer to mean values of the data set.

Table 3. Comparison of surface roughness (R_a) values obtained from experimental and RSM predictions.

Spindle Speed (rpm)	Feed (mm/rev)	Drill Dia (mm)	Drill Type	Experimental R_a (µm)			RSM-Predicted R_a (µm)			Error (%)		
				Al_2O_3	SiC	Neat	Al_2O_3	SiC	Neat	Al_2O_3	SiC	Neat
5500	0.01	8	Step	1.292	1.468	1.843	1.288	1.463	1.834	0.31	0.32	0.46
5500	0.01	8	Core	1.585	1.774	2.51	1.588	1.764	2.494	−0.21	0.54	0.65
5500	0.02	6	Core	1.543	1.723	2.416	1.544	1.710	2.412	−0.09	0.75	0.16
1500	0.01	4	Twist	1.216	1.391	1.893	1.216	1.373	1.891	0.01	1.27	0.10
3500	0.02	6	Step	1.224	1.411	1.751	1.226	1.402	1.745	−0.13	0.67	0.33
1500	0.01	4	Core	1.417	1.576	2.235	1.420	1.589	2.217	−0.19	−0.83	0.82
3500	0.01	6	Step	1.203	1.395	1.735	1.218	1.395	1.734	−1.23	0.01	0.05
1500	0.01	4	Step	1.134	1.317	1.612	1.123	1.320	1.612	0.94	−0.24	0.03
3500	0.02	6	Twist	1.343	1.481	2.067	1.342	1.484	2.053	0.08	−0.18	0.67
5500	0.02	6	Twist	1.371	1.512	2.097	1.369	1.506	2.084	0.11	0.39	0.63
5500	0.03	8	Twist	1.435	1.612	2.192	1.441	1.588	2.194	−0.45	1.49	−0.07
5500	0.03	4	Core	1.478	1.651	2.317	1.486	1.649	2.320	−0.56	0.13	−0.14
1500	0.01	8	Core	1.559	1.731	2.437	1.553	1.724	2.433	0.40	0.40	0.16
3500	0.01	6	Core	1.513	1.684	2.357	1.516	1.680	2.366	−0.20	0.24	−0.39
3500	0.03	6	Step	1.224	1.419	1.768	1.232	1.408	1.758	−0.62	0.79	0.56
1500	0.03	4	Core	1.432	1.61	2.249	1.428	1.608	2.242	0.30	0.14	0.29
5500	0.03	4	Twist	1.294	1.442	1.983	1.297	1.437	1.989	−0.22	0.32	−0.31
3500	0.02	6	Core	1.527	1.694	2.381	1.521	1.690	2.378	0.40	0.26	0.14
5500	0.01	4	Core	1.466	1.637	2.289	1.471	1.629	2.293	−0.35	0.46	−0.19
3500	0.02	6	Core	1.527	1.694	2.381	1.521	1.690	2.378	0.40	0.26	0.14
3500	0.02	8	Step	1.283	1.457	1.824	1.280	1.454	1.820	0.22	0.22	0.20
5500	0.03	8	Core	1.598	1.783	2.533	1.595	1.784	2.517	0.16	−0.06	0.64
3500	0.03	6	Twist	1.362	1.495	2.078	1.348	1.493	2.068	1.03	0.12	0.50
1500	0.03	8	Twist	1.395	1.547	2.149	1.391	1.543	2.140	0.30	0.28	0.43
3500	0.02	6	Core	1.527	1.694	2.381	1.521	1.690	2.378	0.40	0.26	0.14
3500	0.02	6	Twist	1.343	1.481	2.067	1.342	1.484	2.053	0.08	−0.18	0.67
1500	0.03	8	Step	1.275	1.442	1.815	1.267	1.444	1.807	0.64	−0.11	0.42
1500	0.01	8	Step	1.267	1.435	1.794	1.261	1.431	1.786	0.51	0.29	0.45
5500	0.01	8	Twist	1.423	1.585	2.175	1.428	1.568	2.168	−0.35	1.07	0.33
1500	0.02	6	Core	1.492	1.672	2.342	1.497	1.669	2.343	−0.36	0.17	−0.04
3500	0.02	6	Step	1.224	1.411	1.751	1.226	1.402	1.745	−0.13	0.67	0.33
1500	0.03	4	Step	1.146	1.326	1.633	1.138	1.333	1.637	0.73	−0.50	−0.24
3500	0.02	6	Core	1.527	1.694	2.381	1.521	1.690	2.378	0.40	0.26	0.14
1500	0.03	4	Twist	1.227	1.397	1.925	1.230	1.392	1.919	−0.26	0.34	0.29
1500	0.03	8	Core	1.535	1.742	2.454	1.553	1.743	2.455	−1.17	−0.05	−0.04
3500	0.02	8	Core	1.573	1.755	2.479	1.573	1.754	2.474	−0.02	0.06	0.22
3500	0.02	6	Core	1.527	1.694	2.381	1.521	1.690	2.378	0.40	0.26	0.14
3500	0.02	6	Step	1.224	1.411	1.751	1.226	1.402	1.745	−0.13	0.67	0.33

Table 3. *Cont.*

Spindle Speed (rpm)	Feed (mm/rev)	Drill Dia (mm)	Drill Type	Experimental R_a (µm)			RSM-Predicted R_a (µm)			Error (%)		
				Al_2O_3	SiC	Neat	Al_2O_3	SiC	Neat	Al_2O_3	SiC	Neat
3500	0.02	8	Twist	1.412	1.562	2.164	1.412	1.556	2.153	−0.01	0.40	0.50
3500	0.03	6	Core	1.535	1.712	2.397	1.524	1.699	2.391	0.73	0.76	0.26
5500	0.03	8	Step	1.302	1.484	1.862	1.301	1.477	1.857	0.05	0.49	0.26
3500	0.02	6	Twist	1.343	1.481	2.067	1.342	1.484	2.053	0.08	−0.18	0.67
3500	0.02	4	Core	1.451	1.625	2.261	1.452	1.619	2.267	−0.08	0.37	−0.28
5500	0.01	4	Step	1.169	1.362	1.682	1.167	1.353	1.676	0.18	0.69	0.35
3500	0.02	6	Step	1.224	1.411	1.751	1.226	1.402	1.745	−0.13	0.67	0.33
1500	0.02	6	Step	1.192	1.389	1.727	1.206	1.385	1.717	−1.19	0.28	0.60
3500	0.01	6	Twist	1.327	1.472	2.035	1.334	1.474	2.041	−0.53	−0.13	−0.27
3500	0.02	6	Core	1.527	1.694	2.381	1.521	1.690	2.378	0.40	0.26	0.14
5500	0.02	6	Step	1.258	1.429	1.781	1.245	1.418	1.774	1.02	0.78	0.40
3500	0.02	6	Twist	1.343	1.481	2.067	1.342	1.484	2.053	0.08	−0.18	0.67
3500	0.02	6	Twist	1.343	1.481	2.067	1.342	1.484	2.053	0.08	−0.18	0.67
5500	0.03	4	Step	1.187	1.371	1.708	1.188	1.366	1.703	−0.10	0.38	0.31
5500	0.01	4	Twist	1.289	1.423	1.962	1.275	1.418	1.960	1.05	0.37	0.12
3500	0.02	4	Twist	1.245	1.415	1.943	1.256	1.405	1.939	−0.85	0.68	0.21
1500	0.01	8	Twist	1.389	1.525	2.127	1.385	1.524	2.115	0.32	0.09	0.56
3500	0.02	6	Step	1.224	1.411	1.751	1.226	1.402	1.745	−0.13	0.67	0.33
3500	0.02	6	Step	1.224	1.411	1.751	1.226	1.402	1.745	−0.13	0.67	0.33
3500	0.02	6	Twist	1.343	1.481	2.067	1.342	1.484	2.053	0.08	−0.18	0.67
1500	0.02	6	Twist	1.312	1.457	1.994	1.314	1.461	2.023	−0.19	−0.30	−1.43
3500	0.02	4	Step	1.157	1.345	1.651	1.155	1.343	1.656	0.18	0.15	−0.30
Standard deviation				0.133	0.131	0.270	0.133	0.132	0.270	0.494	0.412	0.367

3.1. Analysis of Main Effects Plot

The effect of drilling parameters is represented by the main effects plot for the hybrid nano-composites and the neat CFRP composite, as shown in Figure 4a–c. It can be observed that all the parameters significantly impact the surface roughness of the hole. For the Al_2O_3 hybrid nano-composite, the surface roughness is observed to be at a minimum for lower spindle speed, moderate feed, and lower drill diameter for step drill (Figure 4a). Similar results are noticed for the SiC hybrid nano-composite and neat CFRP composites with minimum surface roughness at lower spindle speed, feed, and drill diameter for step drill (Figure 4b). From the observation made, it is noted that the contribution of spindle speed, drill diameter, and drill type on surface roughness is more as compared to the feed of the drill tool. The surface roughness obtained is lower at a lower spindle speed and drill diameter (Figure 4c). The results are due to the lower heat generated at a lower spindle speed at the tool–workpiece interface.

3.2. ANOVA Analysis

ANOVA analysis (Table 4) shows the influence of process parameters on surface roughness. Table 4 shows that the contribution on surface roughness of drill type is 84.75, 84.70, and 92%, respectively, for the hybrid Al_2O_3 and SiC composites as well as the neat CFRP composite. The next effective parameter having an influence on surface roughness is drill diameter, with a 12.96, 13.10, and 7% contribution, respectively, followed by spindle speed, with a contribution of 1.57, 1.58, and 0.72%, respectively. The contribution of feed on surface roughness is less than 0.2% for all the composites.

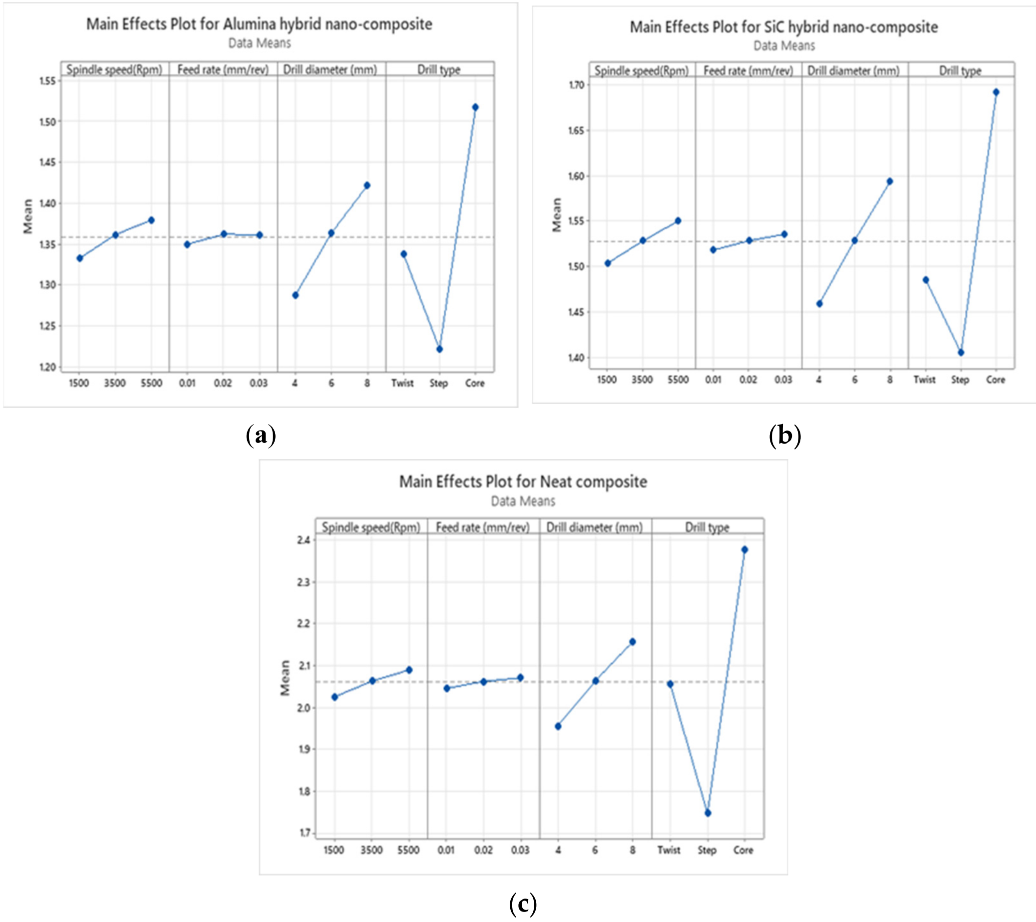

Figure 4. Main effects plot of surface roughness for (**a**) Al_2O_3 hybrid nano-composite, (**b**) SiC hybrid nano-composite, and (**c**) neat CFRP composite.

Table 4. ANOVA table for surface roughness at dry drilling condition.

Source	Al_2O_3 Hybrid Nano-Composite			SiC Hybrid Nano-Composite			Neat CFRP Composite		
	F-Value	*p*-Value	Contribution	F-Value	*p*-Value	Contribution	F-Value	*p*-Value	Contribution
SS (rpm)	271.56	0.000	1.57%	375.32	0.000	1.58%	439.08	0.000	0.72%
F (mm/rev)	17.07	0.000	0.10%	51.13	0.000	0.21%	67.15	0.000	0.11%
DD (mm)	2237.39	0.000	12.96%	3115.81	0.000	13.10%	4294.96	0.000	7.00%
D	7317.61	0.000	84.75%	10,072.15	0.000	84.70%	28,227.18	0.000	92.00%
Square	6.51	0.001	0.11%	0.96	0.423	0.01%	3.88	0.015	0.02%
SS (rpm) × S (rpm)	0.01	0.920	0.05%	0.09	0.768	0.00%	0.19	0.666	0.01%
F (mm/rev) × F (mm/rev)	0.12	0.730	0.01%	0.00	0.948	0.00%	0.09	0.761	0.00%
DD (mm) × DD (mm)	8.96	0.005	0.05%	1.89	0.177	0.01%	5.90	0.019	0.01%
2-Way Interaction	5.16	0.000	0.27%	5.65	0.000	0.21%	6.13	0.000	0.09%
SS (rpm) × F (mm/rev)	1.22	0.277	0.01%	0.02	0.878	0.00%	0.03	0.866	0.00%
SS (rpm) × DD (mm)	6.35	0.016	0.04%	0.22	0.644	0.00%	1.79	0.189	0.00%
SS (rpm) × D	2.58	0.088	0.03%	1.59	0.217	0.01%	1.00	0.378	0.00%
F (mm/rev) × DD (mm)	1.59	0.215	0.01%	0.00	0.975	0.00%	0.31	0.579	0.00%
F (mm/rev) × D	0.53	0.593	0.01%	0.76	0.473	0.01%	0.09	0.910	0.00%
DD (mm) × D	15.53	0.000	0.18%	22.96	0.000	0.19%	25.42	0.000	0.08%
R-square value		**99.76**			**99.82**			**99.93**	
R-square adjusted value		**99.66**			**99.75**			**99.82**	

SS—spindle speed; F—feed; DD—drill diameter; D—drill type.

3.3. Contour Plot Analysis

Contour plots were created to assess surface roughness for hybrid nano-composites and the neat CFRP composite. Figure 5a indicates that, in the case of the Al_2O_3 hybrid nano-composites, superior surface finish in drilled holes can be attained by employing a 4 mm drill diameter, spindle speeds below 1750 rpm, and a feed under 0.02 mm/rev. Similarly, for the SiC hybrid nano-composites (Figure 5b), optimal surface roughness results are achieved with a 4 mm drill diameter, spindle speeds lower than 2000 rpm, and a feed below 0.03 mm/rev. Likewise, for the neat CFRP composite (Figure 5c), a reduction in surface roughness is observed when maintaining spindle speeds below 2000 rpm, a feed under 0.025 mm/rev, and a 4 mm drill diameter.

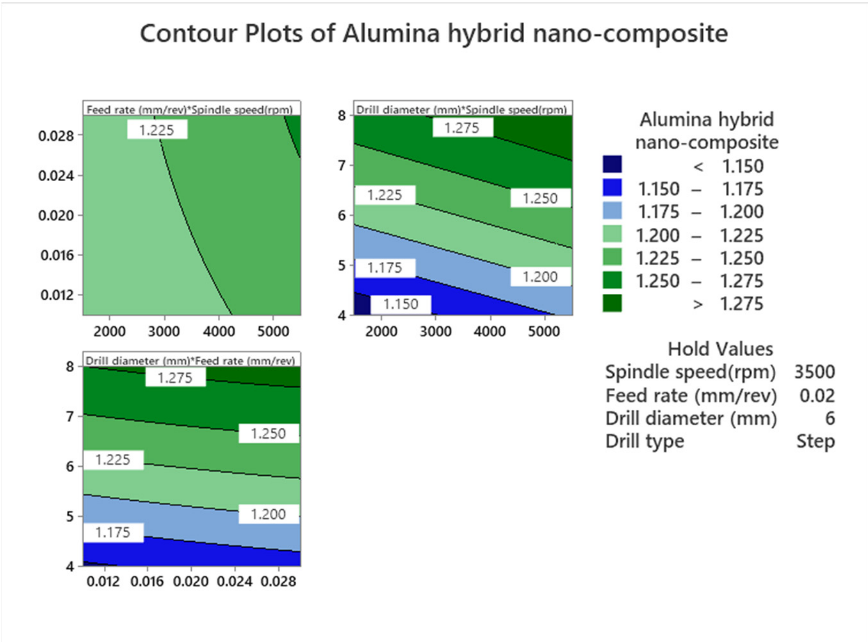

(**a**)

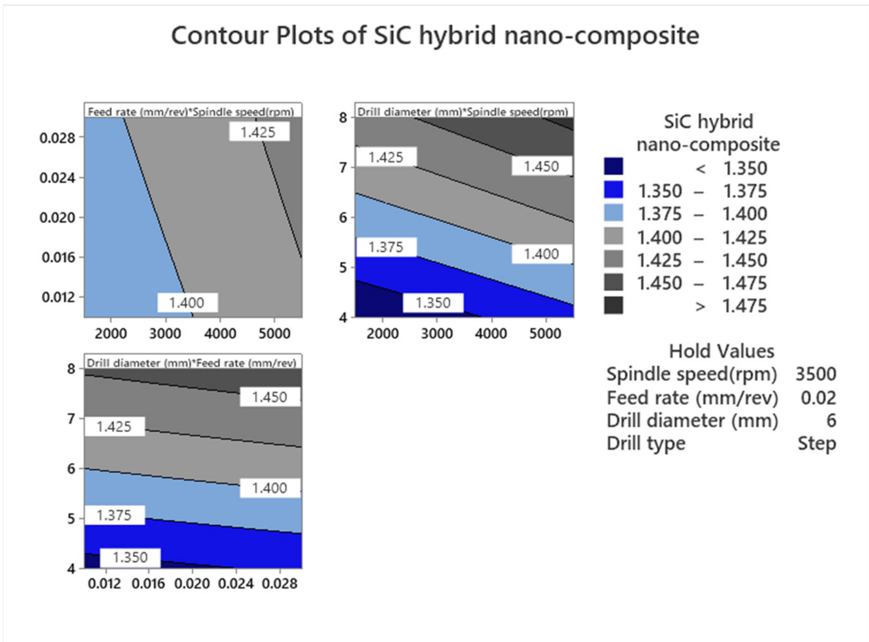

(**b**)

Figure 5. *Cont.*

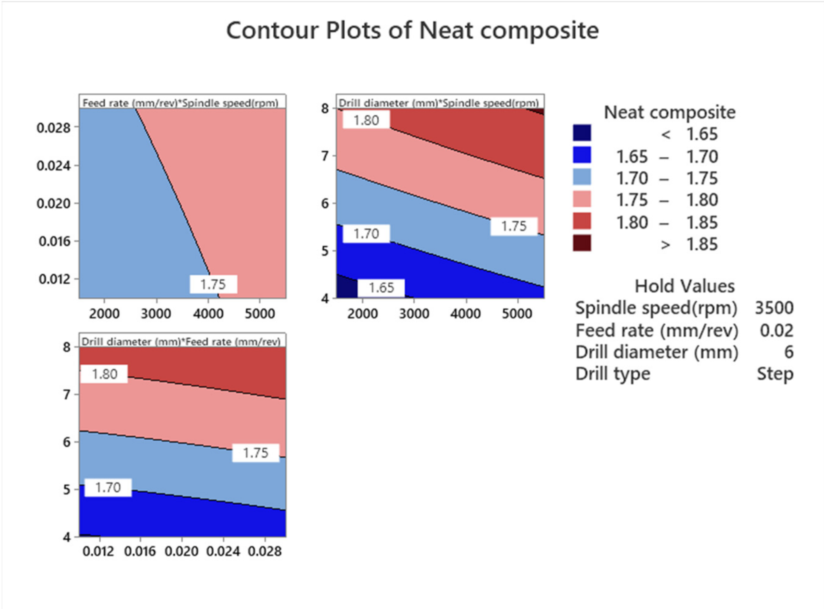

(**c**)

Figure 5. Contour plots of surface roughness for (**a**) Al_2O_3 hybrid nano-composite, (**b**) SiC hybrid nano-composite, and (**c**) neat CFRP composite.

3.4. Optimization of Process Parameters

Optimization techniques have greatly influenced the choice of diverse drilling process parameters. Therefore, optimizing these parameters is imperative in the composite drilling process. Through this optimization, researchers have observed enhancements in the quality of drilled holes and prolonged tool life. Optimization plots obtained for Al_2O_3 and SiC hybrid nano-composites as well as the neat CFRP composite are represented in Figure 6. The optimum cutting conditions for surface roughness are a spindle speed of 1500 rpm, feed of 0.01 mm/rev, drill diameter of 4 mm, and drill type step drill. From the optimization plots, it is observed that the overall desirability index (D) of the surface roughness is 0.9963.

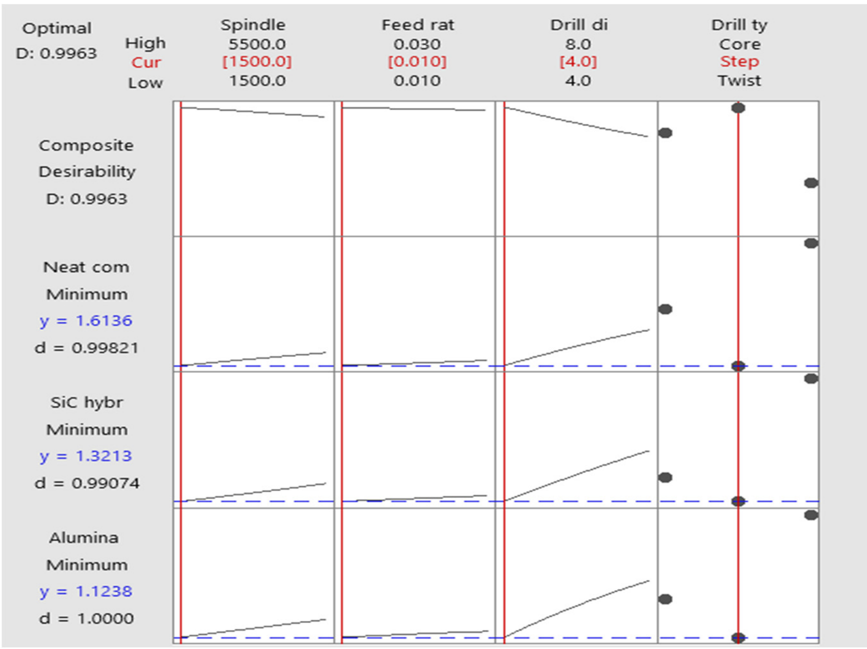

Figure 6. Optimization plots of surface roughness for hybrid nano-composites and neat CFRP composite.

3.5. Confirmation Test

Table 5 represents the confirmation test results, including the experimental and predicted values of the drilling process output variable (surface roughness) of the neat CFRP and hybrid nano-composites. The test was performed using the step, twist, and core drill at the above optimum input process parameters. In the comparison of experimental and predicted values from Table 5, it is observed that the deviation obtained is less than 3%. The values obtained from the confirmation test also showcase that the experimental values obtained are less than the predicted values.

Table 5. Comparison of experimental and RSM-predicted values of surface roughness from the confirmation test performed.

Optimum Input Process Parameters				Composite Type	Experimental Value	RSM-Predicted Value	Error (%)
SS (rpm)	F (mm/rev)	DD (mm)	D				
1500	0.01	4	Step	Al_2O_3 hybrid nano-composite	1.127	1.123	0.28
				SiC hybrid nano-composite	1.332	1.321	0.81
				Neat CFRP composite	1.642	1.613	1.76

SS—spindle speed; F—feed; DD—drill diameter; D—drill type.

3.6. Validation Test

To check the adequacy of the developed regression models from RSM, the validation test was performed based on the different sets of input process parameters, as shown in Table 6, that were not used in performing the experiment earlier but fall within the defined range of experiments. The results obtained from the validation experiment are displayed in Table 7. The experimental and RSM-predicted values appropriately agree with each other, and the percentage error obtained is also represented.

Table 6. Input process parameters selected for validation test.

Experiment No.	Spindle Speed (rpm)	Feed (mm/rev)	Drill Diameter (mm)	Drill Type
1	1500	0.02	4	Twist
2	5500	0.03	6	Step
3	1500	0.01	8	Core

Table 7. Validation test results of surface roughness performed for hybrid nano-composites and neat CFRP composite.

Composite Type	Optimum Input Process Parameters				Experimental Value	RSM-Predicted Value	Error (%)
	SS (rpm)	F (mm/rev)	DD (mm)	D			
Al_2O_3 hybrid nano-composite	1500	0.02	4	Twist	1.224	1.310	7.03
	5500	0.03	6	Step	1.253	1.285	2.55
	1500	0.01	8	Core	1.553	1.502	3.28
SiC hybrid nano-composite	1500	0.02	4	Twist	1.383	1.368	1.08
	5500	0.03	6	Step	1.424	1.345	5.55
	1500	0.01	8	Core	1.724	1.716	0.46
Neat CFRP composite	1500	0.02	4	Twist	1.904	1.853	2.68
	5500	0.03	6	Step	1.787	1.685	5.71
	1500	0.01	8	Core	2.433	2.498	2.67

SS—spindle speed; F—feed; DD—drill diameter; D—drill type.

3.7. Prediction Output

The results obtained from both models (ANN and RF) are presented in Table 8. These tables include predicted R_a values and the errors associated with each prediction for different machining parameters. By analyzing the results obtained from Table 8, the table shows predicted surface roughness (R_a) values from both the artificial neural network (ANN) and random forest (RF) models across diverse drilling scenarios, revealing commendable overall performance. Both models demonstrate their effectiveness in predicting surface roughness, underscoring their utility in understanding complex relationships between drilling parameters and material characteristics. While variations in prediction errors were observed across different combinations of spindle speed, feed, drill diameter, and drill type, the models generally exhibited robust predictive capabilities. This suggests the viability of ANN and RF models in capturing nuanced patterns and trends in surface roughness outcomes, offering valuable insights for optimizing drilling processes in composite materials. The prediction results that were attained showcase that RF outperforms ANN and RSM. Figures 7–9 represent the visual comparison of ANN and RF predictions for Al_2O_3, SiC, and neat CFRP composites. These figures clearly show how well each model performed in predicting surface roughness (R_a) across various conditions. Further, to assess the accuracy of the models, Figures 10–12 illustrate the ANN and RF error predictions concerning the RSM-predicted R_a values. This error analysis provides insights into areas where the models may require refinement and highlights potential areas for improvement. Table 8 also provides an insight into the relative error attained for R_a through the statistical RSM model and machine learning models (ANN and RF). The relative error attained through the implementation of RF is comparatively lower than with ANN and RSM. The reason for the best attainment of results is due to the nature of the support of parallelization (i.e., combining multiple decision trees leads to a reduction of overfitting of the model) and the nature of providing better insights into feature relationships. In this case, ANN is computationally expensive and very sensitive to hypermeters (hyperparameter tuning is challenging).

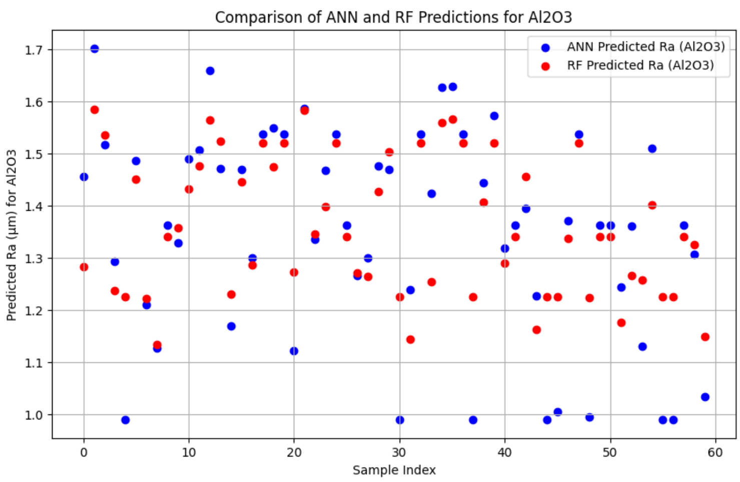

Figure 7. Comparison of ANN and RF predictions of R_a for Al_2O_3 hybrid nano-composite.

Table 8. Comparison of surface roughness values obtained from ANN and RF predictions and relative error scale with respect to RSM prediction.

Spindle Speed (rpm)	Feed (mm/rev)	Drill Diameter (mm)	Drill Type	ANN Predicted Ra (Al_2O_3)	ANN Predicted R_a (Sic)	ANN Predicted R_a (Neat)	RF Predicted R_a (Al_2O_3)	RF Predicted Ra (Sic)	RF Predicted Ra (Neat)	Error ANN (Al_2O_3)	Error ANN (Sic)	Error ANN (Neat)	Error RF (Al_2O_3)	Error RF (Sic)	Error RF (Neat)
5500	0.01	8	1	1.456352	1.571367	2.069188	1.28377	1.45562	1.82663	13.07	7.41	12.82	0.33	0.5	0.4
5500	0.01	8	0	1.702711	1.860966	2.782625	1.5858	1.76628	2.494	7.22	5.5	11.57	0.14	0.13	0
5500	0.02	6	0	1.517819	1.710853	2.380019	1.53677	1.70136	2.39969	1.7	0.05	1.33	0.47	0.51	0.51
1500	0.01	4	2	1.293901	1.492233	1.935694	1.23783	1.38834	1.91747	6.41	8.68	2.36	1.8	1.12	1.4
3500	0.02	6	1	0.990383	1.239939	1.328297	1.226	1.402	1.745	19.22	11.56	23.88	0	0	0
1500	0.01	4	0	1.486014	1.643242	2.497839	1.45184	1.62345	2.27398	4.65	3.41	12.67	2.24	2.17	2.57
3500	0.01	6	1	1.209693	1.279833	1.529487	1.22147	1.39773	1.73778	0.68	8.26	11.79	0.28	0.2	0.22
1500	0.01	4	1	1.127849	1.31431	1.777092	1.13339	1.32767	1.62793	0.43	0.43	10.24	0.93	0.58	0.99
3500	0.02	6	2	1.363549	1.498434	2.009733	1.34172	1.48377	2.0527	1.61	0.97	2.11	0.02	0.02	0.01
5500	0.02	6	2	1.328551	1.388244	2.140685	1.35766	1.49629	2.07034	2.95	7.82	2.72	0.83	0.64	0.66
5500	0.03	8	2	1.490139	1.638373	2.305222	1.43205	1.5773	2.18138	3.41	3.17	5.07	0.62	0.67	0.58
5500	0.03	4	0	1.506602	1.762022	2.394908	1.47622	1.64163	2.30721	1.39	6.85	3.23	0.66	0.45	0.55
1500	0.01	8	0	1.660435	1.980778	2.678755	1.56443	1.75276	2.47348	6.92	14.89	10.1	0.74	1.67	1.66
3500	0.01	6	0	1.470755	1.69469	2.362745	1.52385	1.69013	2.37947	2.98	0.87	0.14	0.52	0.6	0.57
3500	0.03	6	1	1.17039	1.26903	1.51443	1.2299	1.40707	1.75407	5	9.87	13.85	0.17	0.07	0.22
1500	0.03	4	0	1.470053	1.636276	2.388436	1.44558	1.62352	2.26901	2.94	1.76	6.53	1.23	0.97	1.2
5500	0.03	4	2	1.299501	1.497535	2.085393	1.28589	1.42999	1.97819	0.19	4.21	4.85	0.86	0.49	0.54
3500	0.02	6	0	1.53751	1.716213	2.35087	1.521	1.69	2.378	1.09	1.55	1.14	0	0	0
5500	0.01	4	0	1.550188	1.641287	2.362509	1.47563	1.63718	2.30393	5.38	0.75	3.03	0.31	0.5	0.48
3500	0.02	6	0	1.53751	1.716213	2.35087	1.521	1.69	2.378	1.09	1.55	1.14	0	0	0
3500	0.02	8	1	1.122149	1.378606	1.602812	1.27283	1.44604	1.80487	12.33	5.19	11.93	0.56	0.55	0.83
5500	0.03	8	0	1.586365	1.761309	2.602341	1.58391	1.77032	2.49542	0.54	1.27	3.39	0.7	0.77	0.86
3500	0.03	6	2	1.336592	1.438408	2.003405	1.34641	1.49066	2.06407	0.85	3.66	3.12	0.12	0.16	0.19
1500	0.03	8	2	1.468507	1.708831	2.232491	1.39783	1.55035	2.15086	5.57	10.75	4.32	0.49	0.48	0.51
3500	0.02	6	0	1.53751	1.716213	2.35087	1.521	1.69	2.378	1.09	1.55	1.14	0	0	0
3500	0.02	6	2	1.363549	1.498434	2.009733	1.34172	1.48377	2.0527	1.61	0.97	2.11	0.02	0.02	0.01
1500	0.03	8	1	1.26572	1.448932	1.942375	1.27066	1.44708	1.80806	0.1	0.34	7.49	0.29	0.21	0.06
1500	0.01	8	1	1.300653	1.442074	2.009445	1.26474	1.4374	1.79518	3.14	0.77	12.51	0.3	0.45	0.51
5500	0.01	8	2	1.475928	1.613553	2.284549	1.42778	1.56828	2.17075	3.36	2.91	5.38	0.02	0.02	0.13

Table 8. *Cont.*

Spindle Speed (rpm)	Feed (mm/rev)	Drill Diameter (mm)	Drill Type	ANN Predicted Ra (Al_2O_3)	ANN Predicted R_a (Sic)	ANN Predicted R_a (Neat)	RF Predicted R_a (Al_2O_3)	RF Predicted Ra (Sic)	RF Predicted Ra (Neat)	Error ANN (Al_2O_3)	Error ANN (Sic)	Error ANN (Neat)	Error RF (Al_2O_3)	Error RF (Sic)	Error RF (Neat)
1500	0.02	6	0	1.469299	1.639699	2.438071	1.50356	1.67446	2.3521	1.85	1.76	4.06	0.44	0.33	0.39
3500	0.02	6	1	0.990383	1.239939	1.328297	1.226	1.402	1.745	19.22	11.56	23.88	0	0	0
1500	0.03	4	1	1.238851	1.350103	1.749304	1.14411	1.33714	1.64055	8.86	1.28	6.86	0.54	0.31	0.22
3500	0.02	6	0	1.53751	1.716213	2.35087	1.521	1.69	2.378	1.09	1.55	1.14	0	0	0
1500	0.03	4	2	1.423592	1.554698	2.309336	1.25528	1.40284	1.94098	15.74	11.69	20.34	2.06	0.78	1.15
1500	0.03	8	0	1.627112	1.749065	2.587803	1.55896	1.75057	2.46465	4.77	0.35	5.41	0.38	0.43	0.39
3500	0.02	8	0	1.629802	1.823364	2.413243	1.56664	1.7523	2.47004	3.61	3.95	2.46	0.4	0.1	0.16
3500	0.02	6	0	1.53751	1.716213	2.35087	1.521	1.69	2.378	1.09	1.55	1.14	0	0	0
3500	0.02	6	1	0.990383	1.239939	1.328297	1.226	1.402	1.745	19.22	11.56	23.88	0	0	0
3500	0.02	8	2	1.444109	1.531701	2.131912	1.40664	1.5507	2.15089	2.27	1.56	0.98	0.38	0.34	0.1
3500	0.03	6	0	1.572901	1.665941	2.315238	1.52149	1.69308	2.38152	3.21	1.95	3.17	0.16	0.35	0.4
5500	0.03	8	1	1.319746	1.502715	2.03471	1.2895	1.46505	1.83691	1.44	1.74	9.57	0.88	0.81	1.08
3500	0.02	6	2	1.363549	1.498434	2.009733	1.34172	1.48377	2.0527	1.61	0.97	2.11	0.02	0.02	0.01
3500	0.02	4	0	1.395865	1.6597	2.264282	1.45666	1.62613	2.27745	3.87	2.51	0.12	0.32	0.44	0.46
5500	0.01	4	1	1.228172	1.294105	1.741528	1.16271	1.35276	1.67171	5.24	4.35	3.91	0.37	0.02	0.26
3500	0.02	6	1	0.990383	1.239939	1.328297	1.226	1.402	1.745	19.22	11.56	23.88	0	0	0
1500	0.02	6	1	1.005	1.062691	1.638218	1.22567	1.40241	1.74332	16.67	23.27	4.59	1.63	1.26	1.53
3500	0.01	6	2	1.371796	1.362519	1.885923	1.33754	1.47839	2.0446	2.83	7.56	7.6	0.27	0.3	0.18
3500	0.02	6	0	1.53751	1.716213	2.35087	1.521	1.69	2.378	1.09	1.55	1.14	0	0	0
5500	0.02	6	1	0.994668	1.141733	1.600672	1.22443	1.40565	1.74993	20.11	19.48	9.77	1.65	0.87	1.36
3500	0.02	6	2	1.363549	1.498434	2.009733	1.34172	1.48377	2.0527	1.61	0.97	2.11	0.02	0.02	0.01
3500	0.02	6	2	1.363549	1.498434	2.009733	1.34172	1.48377	2.0527	1.61	0.97	2.11	0.02	0.02	0.01
5500	0.03	4	1	1.243497	1.358665	1.831364	1.17602	1.36168	1.68777	4.67	0.54	7.54	1.01	0.32	0.89
5500	0.01	4	2	1.362128	1.524907	2.033442	1.26568	1.41161	1.95207	6.83	7.54	3.75	0.73	0.45	0.4
3500	0.02	4	2	1.130603	1.433997	2.015887	1.25715	1.40698	1.94287	9.98	2.06	3.97	0.09	0.14	0.2
1500	0.01	8	2	1.509835	1.539907	2.257786	1.40215	1.54727	2.14824	9.01	1.04	6.75	1.24	1.53	1.57
3500	0.02	6	1	0.990383	1.239939	1.328297	1.226	1.402	1.745	19.22	11.56	23.88	0	0	0
3500	0.02	6	1	0.990383	1.239939	1.328297	1.226	1.402	1.745	19.22	11.56	23.88	0	0	0
3500	0.02	6	2	1.363549	1.498434	2.009733	1.34172	1.48377	2.0527	1.61	0.97	2.11	0.02	0.02	0.01
1500	0.02	6	2	1.306254	1.408035	1.996562	1.32548	1.46827	2.0353	0.59	3.63	1.31	0.87	0.5	0.61
3500	0.02	4	1	1.034241	1.328674	1.478657	1.14936	1.34206	1.65323	10.46	1.07	10.71	0.49	0.07	0.17

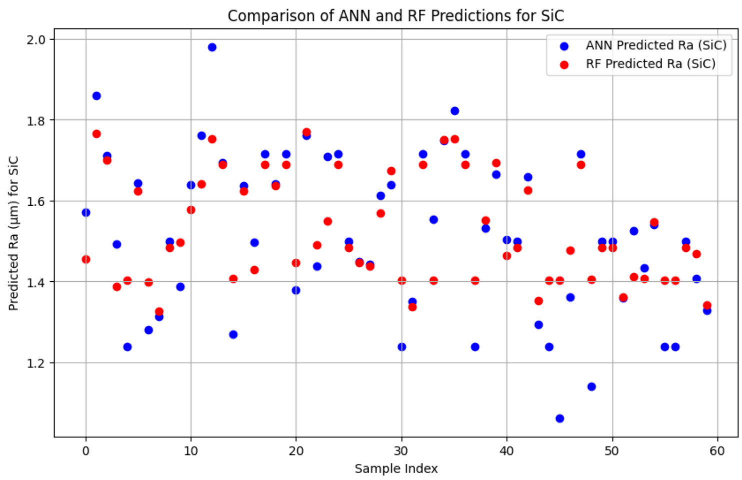

Figure 8. Comparison of ANN and RF predictions of R_a for SiC hybrid nano-composite.

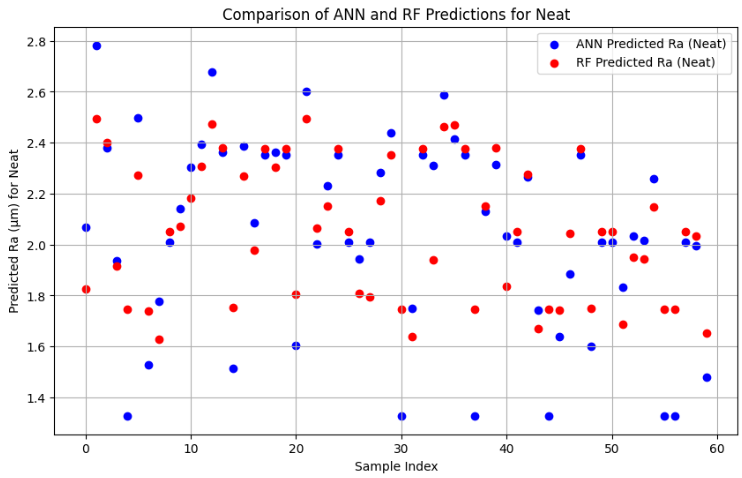

Figure 9. Comparison of ANN and RF predictions of R_a for neat CFRP composite.

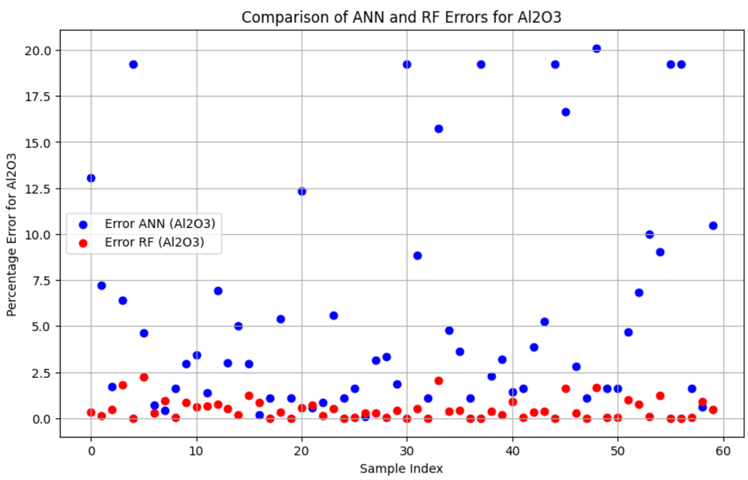

Figure 10. Comparison of ANN and RF error predictions of R_a with respect to RSM-predicted R_a for Al_2O_3 hybrid nano-composite.

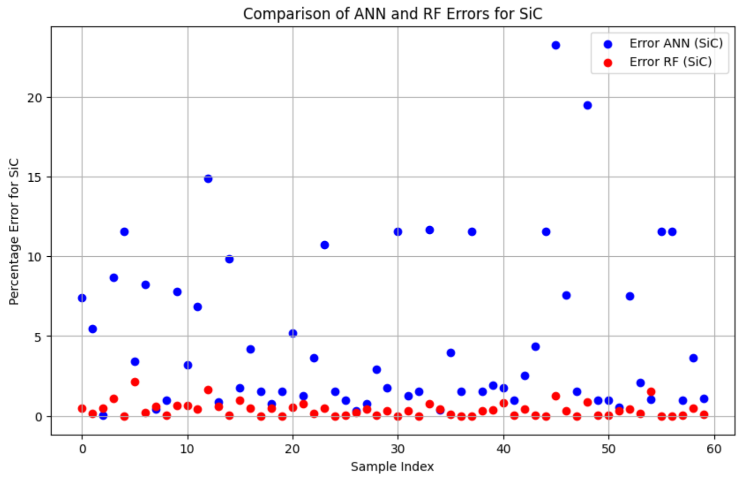

Figure 11. Comparison of ANN and RF error predictions of R_a with respect to RSM-predicted R_a for SiC hybrid nano-composite.

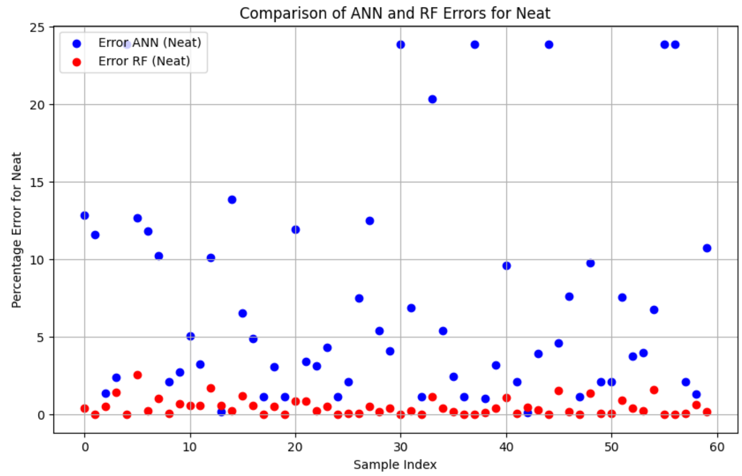

Figure 12. Comparison of ANN and RF error predictions of R_a with respect to RSM-predicted R_a for neat CFRP composite.

4. Conclusions

In this study, an investigation on drilling was conducted using three distinct drill types (step, twist, and core drill) on both neat CFRP and hybrid Al_2O_3 and SiC nano-composites. A total of 60 holes were drilled in each composite type. Based on the experimental findings, the following conclusions can be drawn:

- The input drilling parameters namely spindle speed, feed, drill diameter, and drill type significantly influenced the surface roughness of the investigated nano-composites. The maximum surface roughness value was observed for a higher drill diameter of 8 mm, followed by 6 and 4 mm drill diameters.
- The minimum surface roughness was observed for the Al_2O_3 hybrid nano-composite, followed by the SiC hybrid nano-composite, and maximum surface roughness was noted for the neat CFRP composite.
- Surface roughness increases with increasing spindle speed, feed, and drill diameter, and the drill type step drill has shown better performance in reducing surface roughness.
- ANOVA results indicated that the drill type followed by drill diameter showed a higher percentage contribution to surface roughness.
- The optimization of surface roughness was evaluated using the desirability function approach. From the optimization plot, it was possible to determine the surface roughness by redefining the values of input process parameters within the experimental range.

- The experimental results obtained during the drilling of the hybrid nano-composites and the neat CFRP composite using a step drill, core drill, and twist drill adequately correspond with the RSM-predicted values.
- The comparative analysis of ANN and RF predictions for the hybrid nano-composites and the neat CFRP composite provides visual insights into the performance of each model across different materials.
- The relative error predictions of both ANN and RF concerning the RSM-predicted R_a values, while comparing the results, shows that RF outperforms ANN and RSM due to its interpretability nature.
- The optimized drilling parameters along with the machine learning approach can be employed to other composites, such as glass, Kevlar, and polyimide fiber, for determining their surface roughness qualities.

Author Contributions: Conceptualization, investigation, methodology, writing—original draft (T.N.); Conceptualization, investigation, methodology, writing—original draft (S.M.S.); Conceptualization, writing—review and editing (S.A.); Conceptualization, methodology, writing—review and editing, project administration (N.S.); Conceptualization, writing—review and editing (R.L.M.); Conceptualization, methodology (S.D.S.). All authors have read and agreed to the published version of the manuscript.

Funding: This research received no external funding.

Data Availability Statement: Data are contained within the article.

Conflicts of Interest: The authors declare no conflict of interest.

References

1. Ze, G.K.; Pramanik, A.; Basak, A.K.; Prakash, C.; Shankar, S.; Radhika, N. Challenges Associated with Drilling of Carbon Fiber Reinforced Polymer (CFRP) Composites—A Review. *Compos. Part C Open Access* **2023**, *11*, 100356. [CrossRef]
2. Xu, J.; Yin, Y.; Paulo Davim, J.; Li, L.; Ji, M.; Geier, N.; Chen, M. A Critical Review Addressing Drilling-Induced Damage of CFRP Composites. *Compos. Struct.* **2022**, *294*, 115594. [CrossRef]
3. Nuhiji, B.; Swait, T.; Bower, M.P.; Green, J.E.; Day, R.J.; Scaife, R.J. Tooling Materials Compatible with Carbon Fibre Composites in a Microwave Environment. *Compos. Part B Eng.* **2019**, *163*, 769–778. [CrossRef]
4. Kaybal, H.B.; Ulus, H.; Demir, O.; Şahin, Ö.S.; Avcı, A. Effects of Alumina Nanoparticles on Dynamic Impact Responses of Carbon Fiber Reinforced Epoxy Matrix Nanocomposites. *Eng. Sci. Technol. Int. J.* **2018**, *21*, 399–407. [CrossRef]
5. Li, N.; Li, Y.; Zhou, J.; He, Y.; Hao, X. Drilling Delamination and Thermal Damage of Carbon Nanotube/Carbon Fiber Reinforced Epoxy Composites Processed by Microwave Curing. *Int. J. Mach. Tools Manuf.* **2015**, *97*, 11–17. [CrossRef]
6. Sheikh-Ahmad, J.Y. *Machining of Polymer Composites*; Springer: Berlin/Heidelberg, Germany, 2009; Volume 387355391, ISBN 9780387355399.
7. Wetzel, B.; Haupert, F.; Qiu Zhang, M. Epoxy Nanocomposites with High Mechanical and Tribological Performance. *Compos. Sci. Technol.* **2003**, *63*, 2055–2067. [CrossRef]
8. De Cicco, D.; Asaee, Z.; Taheri, F. Use of Nanoparticles for Enhancing the Interlaminar Properties of Fiber-Reinforced Composites and Adhesively Bonded Joints—A Review. *Nanomaterials* **2017**, *7*, 360. [CrossRef]
9. Mohanty, A.; Srivastava, V.K.; Sastry, P.U. Investigation of Mechanical Properties of Alumina Nanoparticle-loaded Hybrid Glass/Carbon-fiber-reinforced Epoxy Composites. *J. Appl. Polym. Sci.* **2014**, *131*, 39749. [CrossRef]
10. Swain, P.T.R.; Biswas, S. Effect of Moisture Absorption on the Mechanical Properties of Ceramic Filled Jute/Epoxy Hybrid Composites. *IOP Conf. Ser. Mater. Sci. Eng.* **2017**, *178*, 12010. [CrossRef]
11. Shahabaz, S.M.; Shetty, P.K.; Shetty, N.; Sharma, S.; Divakara Shetty, S.; Naik, N. Effect of Alumina and Silicon Carbide Nanoparticle-Infused Polymer Matrix on Mechanical Properties of Unidirectional Carbon Fiber-Reinforced Polymer. *J. Compos. Sci.* **2022**, *6*, 381. [CrossRef]
12. Shahabaz, S.M.; Mehrotra, P.; Kalita, H.; Sharma, S.; Naik, N.; Noronha, D.J.; Shetty, N. Effect of Al_2O_3 and SiC Nano-Fillers on the Mechanical Properties of Carbon Fiber-Reinforced Epoxy Hybrid Composites. *J. Compos. Sci.* **2023**, *7*, 133. [CrossRef]
13. Davim, J.P.; Reis, P.; Antonio, C.C. Experimental Study of Drilling Glass Fiber Reinforced Plastics (GFRP) Manufactured by Hand Lay-Up. *Compos. Sci. Technol.* **2004**, *64*, 289–297. [CrossRef]
14. Tsao, C.C.; Hocheng, H.; Chen, Y.C. Delamination Reduction in Drilling Composite Materials by Active Backup Force. *CIRP Ann.* **2012**, *61*, 91–94. [CrossRef]
15. Rathod, D.; Rathod, M.; Patel, R.; Shahabaz, S.M.; Shetty, S.D.; Shetty, N. A Review on Strengthening, Delamination Formation and Suppression Techniques during Drilling of CFRP Composites. *Cogent Eng.* **2021**, *8*, 1941588. [CrossRef]

16. Palanikumar, K.; Davim, J.P. Mathematical Model to Predict Tool Wear on the Machining of Glass Fibre Reinforced Plastic Composites. *Mater. Des.* **2007**, *28*, 2008–2014. [CrossRef]
17. Ameur, M.F.; Habak, M.; Kenane, M.; Aouici, H.; Cheikh, M. Machinability Analysis of Dry Drilling of Carbon/Epoxy Composites: Cases of Exit Delamination and Cylindricity Error. *Int. J. Adv. Manuf. Technol.* **2017**, *88*, 2557–2571. [CrossRef]
18. Feng, Z.; Gani, H.; Damayanti, A.D.; Gani, H. An Explainable Ensemble Machine Learning Model to Elucidate the Influential Drilling Parameters Based on Rate of Penetration Prediction. *Geoenergy Sci. Eng.* **2023**, *231*, 212231. [CrossRef]
19. Solati, A.; Hamedi, M.; Safarabadi, M. Combined GA-ANN Approach for Prediction of HAZ and Bearing Strength in Laser Drilling of GFRP Composite. *Opt. Laser Technol.* **2019**, *113*, 104–115. [CrossRef]
20. Murthy, B.R.N.; Rodrigues, L.L.R.; Sharma, N.Y.; Anjaiah, D. Influence of Process Parameters on the Quality of Hole in Drilling of GFRP Composites-an Experimental Investigation Using DOE. In Proceedings of the 2010 International Conference on Mechanical and Electrical Technology, Singapore, 10–12 September 2010; IEEE: Piscataway, NJ, USA, 2010; pp. 87–90.
21. Montgomery, D.C. *Design and Analysis of Experiments*; John Wiley & Sons: Hoboken, NJ, USA, 2017; ISBN 1119113474.
22. Jayabal, S.; Natarajan, U. Optimization of Thrust Force, Torque, and Tool Wear in Drilling of Coir Fiber-Reinforced Composites Using Nelder–Mead and Genetic Algorithm Methods. *Int. J. Adv. Manuf. Technol.* **2010**, *51*, 371–381. [CrossRef]
23. Enemuoh, E.U.; El-Gizawy, A.S.; Okafor, A.C. An Approach for Development of Damage-Free Drilling of Carbon Fiber Reinforced Thermosets. *Int. J. Mach. Tools Manuf.* **2001**, *41*, 1795–1814. [CrossRef]
24. Karthikeyan, R.; Jaiganesh, S.; Pai, B.C. Optimization of Drilling Characteristics for Al/SiC p Composites Using Fuzzy/GA. *Met. Mater. Int.* **2002**, *8*, 163–168. [CrossRef]